Physica B 615 (2021) 413063

Contents lists available at ScienceDirect

Physica B: Physics of Condensed Matter

journal homepage: www.elsevier.com/locate/physb

The electronic transport properties of SWCNTs under the influence of deformation and a magnetic field

Ali A. Abdulhussain, M.J. Majid *

Department of Physics, College of Education for Pure Sciences, University of Basrah, 61004, Basrah, Iraq

ARTICLE INFO

Keywords:
Conductance
I–V Characteristics
SWCNT
Deformation
Magnetic field

ABSTRACT

The conductance and *I–V* characteristics are presented for SWCNTs under the influence of the longitudinal magnetic field and mechanical deformation. The electrical properties of zig-zag (9,0), armchair (10,10) and chiral (15,6) SWCNTs have been studied analytically at zero temperature under the influence of the uniaxial and torsional deformation in addition to the longitudinal magnetic field. The calculations of current and conductance are carried out by using the Landauer-Büttiker formula, which is expressed in term of the energy spectrum expression, that derived by using the tight binding approximation. It is shown that the behavior of the conductance and *I–V* characteristics of SWCNTs can be modified and controlled under the effect of the mechanical deformation and magnetic field. Thus, the magnetic field may enhance the effect of the mechanical deformation and improve the electronic properties, or may be cancelled it depending on the chirality of SWCNTs or the type of deformation.

1. Introduction

One of the most important carbon nanostructures is the carbon nanotubes, which are discovered by Iijima in 1991 [1]. These various structures arise due to the ability of the carbon atom to form hybridized orbitals and then produce the relative formation of stable structures with different coupling configurations. The carbon nanotubes are usually divided into two categories: single-walled nanotubes (SWCNTs) and multi-walled nanotubes (MWCNTs). A single-walled carbon nanotube consists of one cylindrical structure formed by rolling a graphene sheet, while multi-walled nanotubes consist of concentric embedded cylinders with different radiuses, separated by a distance between the walls that are controlled by van der Waal forces. The diameters of carbon nanotubes range from 0.3 nm for the smallest single-walled carbon nanotubes to 200 nm for the largest multi-walled carbon nanotubes [2,3].

In addition, several unique properties and measurements such as, dependency of the energy gap on the symmetry of the CNT and the high strength proved the possibility of using these structures in the nanoelectronics and nanomechanics. Many experiments have been motivated by extensive atomistic studies on the relationship between the electronic transport property and the mechanical deformation in all allotropes of carbon nanostructures.

Numerous theoretical and experimental studies were devoted to controlling the *I–V* characteristics and the conductance in the carbon nanostructures. Many methods are used to enhance the electrical properties in the carbon nanostructures, such as: the doping of impurities, mechanical deformation and the exposure to the external electric or magnetic field. Ning Ma et al. have showed the effects of mechanical deformation on the magnetotransport of graphene in the presence of a perpendicular magnetic field with a 1D electrostatic periodic potential [4]. A systematic study of the variation in *I–V* characteristics of single-walled carbon nanotube thin-film transistors has been conducted theoretically and experimentally by Jialuo Chen et al. [5]. On the other hand, an experimental study that modifies the electronic properties of the single-walled carbon nanotube (SWCNT) on the hexagonal boron nitride by using the doping via high-pressure H_2 exposure is reported by H. Kang et al. [6]. Olga E. Glukhova et al. presented a new universal method to calculate the electrical conductance in *2D* materials [7]. The wrapping of single-walled carbon nanotubes (SWCNTs) with ionic surfactants has been studied by Gwyn. P. Evans et al. [8], they discovered that it leads to induce a switch in the behavior of the conductance-humidity of single-walled carbon nanotube networks. The Landauer-Büttiker formula has also been considered theoretically to calculate the conductance of an armchair graphene nanoribbon with an arbitrary uniaxial deformation [9]. In Ref. [10], the electronic properties of two dimension graphene are investigated under the influence of

* Corresponding author. Tel.: +9647705606144.
E-mail address: majid.jasim.nano@gmail.com (M.J. Majid).

https://doi.org/10.1016/j.physb.2021.413063
Received 21 March 2020; Received in revised form 3 April 2021; Accepted 11 April 2021
Available online 20 April 2021

deformation through the tight-binding approximation. In a wide range spectrum, the energy band structure and the density of state (DOS) have been computed numerically.

The change in the electrical properties of zigzag carbon nanotubes (10,0) under the effect of uniaxial compression and tensile deformation has been done to modify the band gap by using the calculations of the density functional theory (DFT). Aditya I. D. et al. Emphasizes that the energy gap of zigzag (10,0) CNTs decreases as the deformation increases for both uniaxial compression and tensile deformation [11].

The effects of the diameter and length in the single-walled carbon nanotube (SWCNT) structures on the transparent conductivity of their network films have been investigated by Yuki Kuwahara *el. al.* [12]. The first principles calculations were used to study the substitutional impurities in zigzag (10,0) carbon nanotubes by Fahdzi Muttaqien et al. [13]. It has illustrated how the impurities such as silicon atom can modify the energy gap of zigzag (10,0) CNT. It is depicted that the energy gap is equal to 0.19 eV, i.e. it is narrower than that of CNT without impurities. Furthermore, in the case of substitution by an arsenic or gallium atom, the zigzag CNT becomes metallic. Recently, the relation between the electrocatalytic processes and band structure has been proposed in the carbon nanostructures. Szroeder et al. have demonstrated that the band structure of graphene is sensitive to the mechanical deformations of lattice and to the effect of defects [14]. However, Ref. [15] investigated the electronic transport properties of zig-zag, armchair and chiral SWCNTs theoretically at zero temperature under the influence of the uniaxial and torsional deformation.

The manipulation of the energy gap width of SWCNTs can be controlled through the combination of the uniaxial and torsional deformation with the external magnetic field. The main objective of our study is to provide insights about the manipulating the energy gap in the SWCNTs by applying the mechanical deformation and magnetic field simultaneously, a matter leads to change the conductance and *I–V* characteristics, which can be useful in the future applications of SWCNTs in nano-electronic and nano-optical devices.

In the first section of our paper, we review the previous works about the mechanical deformation and the electronic properties of the carbon nanostructures in the presence of the electrical or magnetic fields and the effect of impurities. In the next section, the mathematical details are described for the purpose of clarifying the calculations. The third section discusses our results for armchair (10,10), zig-zag (9,0) and chiral (15,6) SWCNTs. The conclusions are presented in the final section.

2. Computational details

In the proposed one-parameter model of the tight binding approximation, the electronic spin is not taken into account, thus, the quantum state of the electron is determined through two quantum numbers: the magnetic quantum number $\boldsymbol{m}$ and the longitudinal wave vector $\boldsymbol{k}$, while the energy spectrum of electron is determined by the following formula [16]:

$$E_k^m = \pm \left| \sum_{j=1}^{2} \beta_j \, e^{-\,i\,\left(m\delta\, x_j + k\delta\, y_j\right)} + \beta_3 \, e^{-im\,(\delta\, x_1 + \delta\, x_2)\,-ik(\delta\, y_1 + \delta\, y_2)} \right| \quad (1)$$

where β_j ($j = 1,2,3$) represents the matrix elements for the amplitudes of the electron hopping through the nearest neighbors in the atomic structure of the CNT [17,18]:

$$\beta_j = t_G \exp\left(-\beta \left(-1 + \left|\delta_j^{'}\right| \,/\, a_0 \right) \right), \; j = 1,2,3 \quad (2)$$

where $\beta \cong 3.37$ is the Grüneisen parameter. The energy parameter or the hopping integral $t_G = 2.67$ eV, $a_0 = 1.42A^o$ is the distance between two of the nearest atoms in the undeformed structure of CNT and $\delta_j^{'}$ represents the distance which connect any atom with the nearest three neighbors of its deformed counterpart. For the tiny limit of the mechanical deformation, we have $\delta_j^{'} = \left|\delta_j\right| . \left(u\left(r + \delta_j\right) - u\left(r\right)\right)$.

Our present paper mainly focuses on the study of the transport properties dependence for SWCNTs including the *I–V* characteristics and the conductance on the applied magnetic field parallel to its axis. However, this is related to the Aharonov- Bohm effect and subsequently the original periodic boundary condition for CNTs $C_h \bullet k = 2\pi m$ will be modified by the phase factor $\Phi e/\hbar$, where Φ is the magnetic flux and e is the elementary charge.

The flux Φ of the applied magnetic field through the cross section of the CNT with radius R is given as a function of the magnetic induction B as follows: $\Phi = \pi R^2 B$. Then, the boundary condition can be modified as follows [19,20]:

$$\vec{c}_h \,.\, \vec{k} = 2\pi\, q + eB\frac{\pi R^2}{\hbar} \quad (3)$$

The effect of the applied magnetic field on the CNT can be revealed in the energy spectrum formula via the replacement of the magnetic quantum number m by $m + \varphi$, where φ is equal to Φ/Φ_0, $\Phi_0 = c\hbar/e$ which represents the magnetic quantum flux and c is the light velocity. Subsequently, formula (1) can be rewritten to include the effect of the magnetic field as follows:

$$E_k^m = \pm \left| \sum_{j=1}^{2} \beta_j \, e^{-\,i\,\left((m+\varphi)\,\delta\, x_j + k\delta\, y_j\right)} + \beta_3 \, e^{-i(m+\varphi)\,(\delta\, x_1 + \delta\, x_2)\,-\,ik(\delta\, y_1 + \delta\, y_2)} \right| \quad (4)$$

It is known that the conductance refers to the transmission of electrons through the electronic device at the Fermi energy level, broadened by the finite thermal width of the Fermi function. The conductance of the one dimensional structures such as CNT is represented in the Landauer-Büttiker formula as follows [20]:

$$G = \frac{4e^2}{h} \sum_j \frac{df\,\left[(E - E_F)/k_B T\right]}{dE}\, \xi_j\,(E)\, dE \quad (5)$$

where $\xi_j\,(E)$ is the transmission of the subband state at the Fermi level and $df\,(\ldots)/dE$ is the derivative of the Fermi function to the energy. When the Fermi energy is in the middle of the band gap, $\xi_j(E_F) = 0$, the conductance is determined by the thermal activation at the ends of the Fermi function. When E_F lies within a conduction or valence band, the conductance is determined by the transmission properties of the CNTs and the contacts. If the CNTs possess a ballistic transport and has perfect contacts, eq. (5) is reduced to a quantized conductance by the amount $4e^2/h$. The conducting CNTs approach to the quantized conductance value at room temperature [20]. Consequently, the conductance of CNTs without scattering (i.e. in the ballistic regime) corresponds to the number of conducting channels multiplied by the conductance quantum $G_o = 2e^2/h$, which may be possible to change under the effect of deformation.

Our calculations are based on the formalism constructed by Savinskii et al. [21] as well as the dispersion relation which is expressed in the tight binding approximation to investigate the behavior of *I–V* characteristics and the conductance of armchair, zig-zag and chiral CNTs placed in the uniform magnetic field in addition to the effect of the uniaxial tension and torsional deformation.

Let us assume that the two ends of the CNT are connected to the contacts which are supplied by the voltage. Furthermore, suppose that the movement of the electron in the CNT from one end to the other is ballistic, the mean free path of the electron is much larger than the length of the CNT in the present study. The difference between the values of the chemical potentials for two ends of the CNT is equal to eV at the thermodynamic equilibrium. Thus, the electric current will be emerging due to the variation in the electronic fluxes of these ends [21].

The CNT can carry the electronic flux from one end to the other passing through an arbitrary cross-section of its structure, which can be represented as follows [21]:

$$J = \frac{2e}{\hbar L} \sum_{m,k} \frac{\partial E_k^m}{\partial k} f_k^m \quad (6)$$

Where E_k^m refers to the dispersion energy of the CNT, the filling probability of any quantum state is given by the Fermi-Dirac function f_k^m as follows:

$$f_k^m = \left(1 + \exp\left[\frac{E_k^m - \mu}{k_B T}\right]\right)^{-1} \quad (7)$$

k_B and μ are the Boltzmann constant and the chemical potential, respectively. In our consideration, the summation is achieved over the valence and conduction bands in the energy spectrum E_k^m for all allowed quantum states included in these bands.

At zero temperature, the electronic flux is then described by means of a simple formula, where the Fermi-Dirac function is given by the step function $f_k^m = \Theta(\mu - E_k^m)$. An electric current will be generated in the CNT due to the electronic flux difference at the left and right ends of it, which is given by:

$$I = J_L - J_R = \frac{2e}{h} \sum_m (eV - E_{\min}^m)\, \Theta(eV - E_{\min}^m) \quad (8)$$

where $E_{\min}^m$ is the minimum value of the energy in the conduction band for the spectrum of the CNT at a given value of the magnetic quantum number m. The summation in Eq. (8), tends to include all the states for each value of the magnetic quantum numbers m in the valence band which ensures the satisfaction of the condition $E_{\min}^m \leq eV$.

On the other hand, the expression for the conductance in the CNT can be obtained from Eq. (8) at zero temperature straightforwardly, as follows [21]:

$$G = \frac{I}{V} = \frac{2e^2}{h} \sum_m \left(1 - \frac{E_{\min}^m}{eV}\right) \Theta(eV - E_{\min}^m) \quad (9)$$

Two regimes of the mechanical deformation have been devoted in our present paper to investigate the uniaxial tension along the axis of CNT and the torsional deformation in addition to the effect of external magnetic field. In our theoretical consideration, the deformation is based on the analysis of Hooke's law, which is given in terms of the deformation parameter γ; here, $\gamma = (L - L_0)/L_0$, where L and L_o are the length of the deformed and undeformed CNT, respectively [22].

The parameters of the helical operators of a deformed CNT in the longitudinal and transverse orientation are determined as follows: $\delta' x_j \rightarrow \delta x_j + \delta y_j \times \gamma_1/R$ and $\delta' y_j \rightarrow \delta y_j \times (1 + \gamma_2)$, respectively [23], where γ_1 and γ_2 are the dimensionless parameters of the torsional and uniaxial deformation, respectively. Here, it is convenient to consider the value of parameter $\gamma_1 = 0$ for the uniaxial deformation. The torsional deformation is a relative cross sectional shift along the axis of the CNT and it can be described by the angle γ_1, we therefore assume the parameter $\gamma_2 = 0$ and the positive values of γ_1 is considered, which means that the torsional deformation is relatively clockwise with respect to one specific direction of the CNT axis.

3. Results and discussion

We have first investigated the *I–V* characteristic of armchair (10,10) CNT, as illustrated in Fig. (1), without and under the influence of the mechanical deformation in the absence and presence of the magnetic field. At zero magnetic flux and in the absence of the mechanical

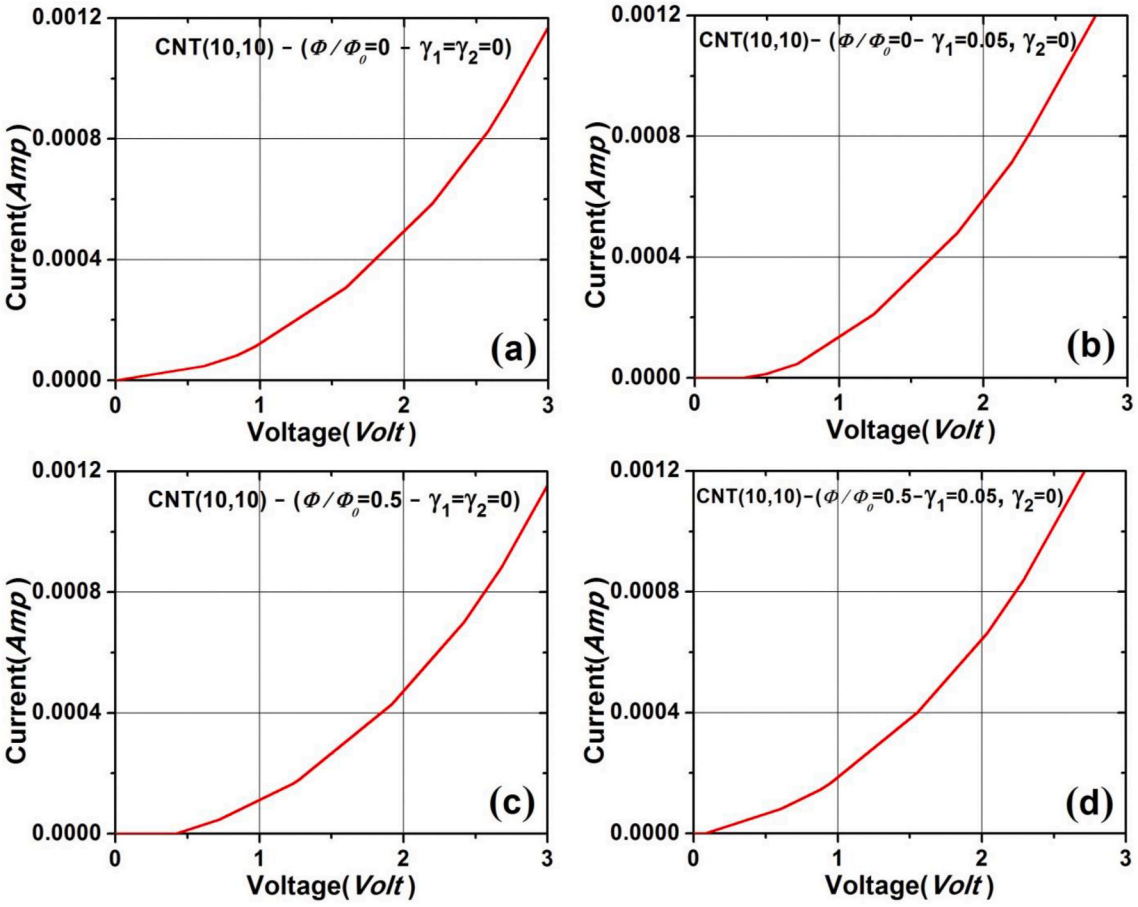

Fig. 1. *I–V* characteristics for armchair (10,10) CNT: undeformed with $\Phi/\Phi_0 = 0$ (a), under torsional deformation with $\Phi/\Phi_0 = 0$ (b), undeformed with $\Phi/\Phi_0 = 0.5$ (c) and under torsional deformation with $\Phi/\Phi_0 = 0.5$ (d).

deformation, it is observed from Fig. 1(a) that the current increases linearly by increasing the voltages. Then, two kinks emerge at the voltages of 0.65 V and 1.6 V, respectively, which correspond to the opening of new channels for electrons. Our results coincide with the previous study of the armchair (5,5) CNT [15]. It can be noticed from Fig. 1(b) that the armchair (10,10) CNT behaves like a semiconductor under the torsional deformation, where the current grows at the threshold voltage and becomes equal to 0.34 V for the torsional parameter in order of $\gamma_1 = 0.05$ with the appearance of the two kinks at the voltages 0.72 V and 1.8 V, respectively. All of these changes in the electronic properties are closely related to the process of breaking the transitional symmetry in the lattice of the CNT. Fig. 1(c) illustrates the influence of applying the magnetic field to *I–V* characteristics for undeformed armchair (10,10) CNT, at a magnetic flux of 0.5. It can be seen that the first conduction channel is opened at the threshold voltage 0.426 V, that corresponds to the quantum magnetic number $m = 10$ in the band structure diagram. We can also see the appearance of the kinks at the voltage values 0.75 V and 1.28 V. Therefore, it means that the value of the threshold voltage increases from 0.34 V to 0.426 V as the energy gap increases under the influence of the magnetic field. Also by comparing Fig. 1(b) with Fig. 1(c), we obtained that the deformation effect are comparable to that of the magnetic field for the armchair (10, 10) CNT. On the other hand, when the torsional deformation and magnetic field are applied together to the armchair (10,10) CNT, it is observed from Fig. 1(d) that the electrical current begins to appear at the threshold voltage 0.087 V, with two of the conduction channels at the voltage values 0.9 V and 1.6 V, respectively. Besides that, we can also see from Fig. 1(d) that the applied magnetic field eliminates the effect of the torsional deformation on the armchair (10,10) CNT. Thus, the conducting armchair (10,10) CNT can be modified to become a semiconducting CNT due to the magnetic field, which is equivalent to the effect of the deformation. Both effects are based on the reduction in the available channels for the electronic transport; hence, the current does not appear until the threshold voltage of order of 0.45 V is available. The *I–V* characteristic curve of armchair (10,10) CNT has not been affected by applying the uniaxial deformation, in the sense that the electronic properties of this type of the tubes unchangeable under the influence of uniaxial deformation in the presence or absence of a magnetic field.

The behavior of the conductance has been studied as a function of the voltage and it is presented in terms of units $2e^2/h$ for armchair (10,10) CNT as depicted in Fig. 2, which shows it under the effect of the magnetic field and the torsional deformation in different values of the parameter γ_1 (0.02, 0.04 and 0.05). As shown in Fig. 2(a), the conductance decreases with the increase in the torsional deformation due to the band gap opening between the valence and conduction bands. It is noted that the behavior of the conductivity curves differ at the voltage values ranging between (0.01–0.75) V, with a slight difference in its behavior when the voltage values range between (0.75–3) V. It is also clear that there is a very slight difference between the conductance values at the parameters ($\gamma_1 = 0.04$ and 0.05), with great similarity in their behavior. The effects of the magnetic field and the deformation on the behavior of the conductance can be seen more clearly in Fig. 2(b), where it reduces the amount of the conductance by decreasing the mechanical deformation.

The conductance has been studied as a function of the uniaxial tension and torsional deformation as illustrated in Fig. 2(c). It is shown that

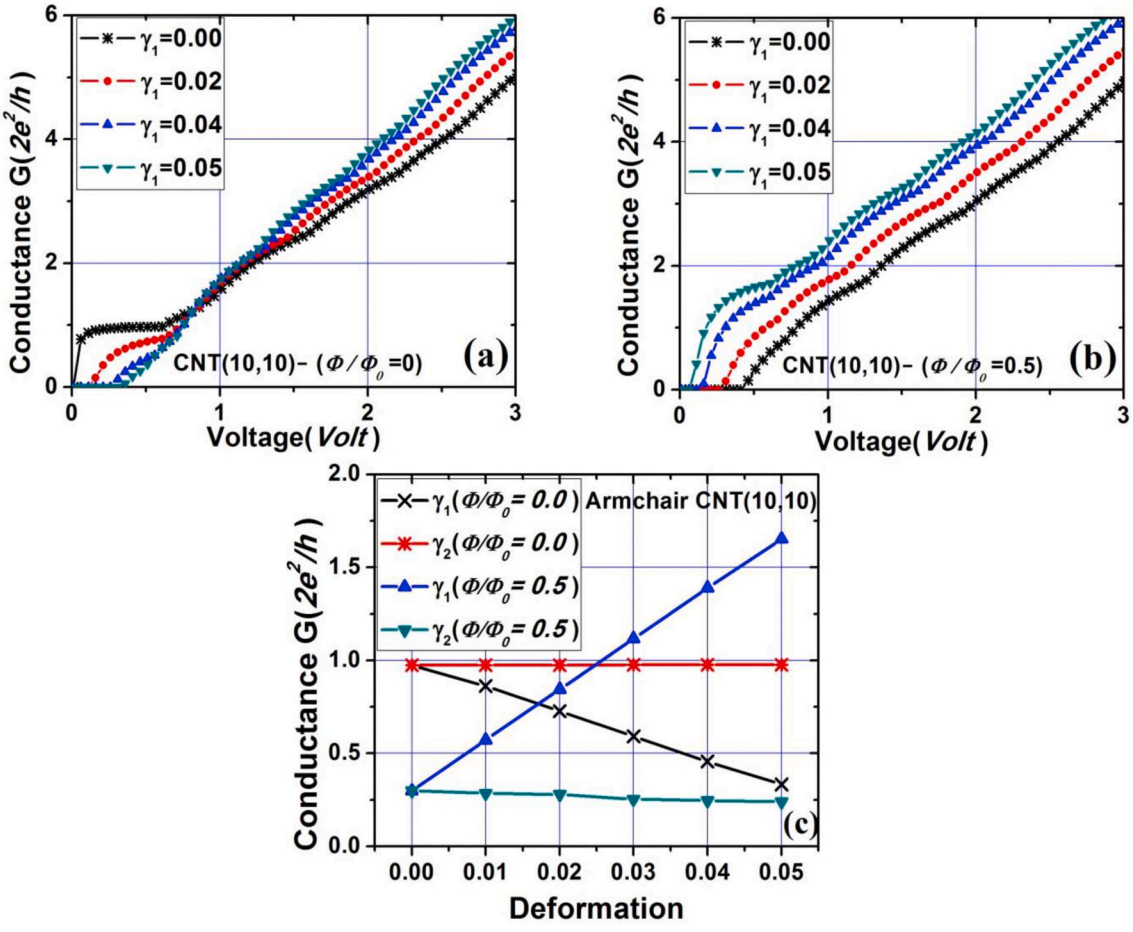

Fig. 2. The conductance dependence on the voltage for armchair (10,10) CNT under torsional deformation without magnetic flux (a), with magnetic flux (b) and the conductance dependence on the deformation parameters without and with magnetic flux (c).

the conductance does not change under the uniaxial tension in the absence of the magnetic field due to the preservation of the mirror symmetry, while it decreases by increasing the torsional deformation due to disappearance of some of the conducting channels. Furthermore, the conductance increases linearly with the applied deformation, (i.e. by increasing the torsional deformation parameter γ_1 in the presence of the magnetic fields), while it does not change significantly with increasing the uniaxial tension parameter γ_2 as presented in Fig. 2(c). This may occurs because some of the conducting channels can be blocked or opened and hence they lead to reducing or enlarging the energy gap in the case of the torsional deformation, respectively.

Specifically, it is well known that one effect may eliminate the influence of the other, and the electronic characteristics of the deformed CNT under the effect of magnetic field nearly remain unchanged as for the undeformed CNT. On the other hand, the uniaxial deformation is not relevant to the effect of the magnetic field. The above behavior can be understood and interpreted as a reverse mutual effect for both the magnetic field and the elastic deformation on the shift direction of the Dirac points in the reciprocal lattice of CNT.

Fig. 3 presents the *I–V* characteristic of zig-zag (9,0) CNT for the undeformed, under torsional deformation, under uniaxial deformation in the absence and presence of a magnetic field. It is well known that the zig-zag (9,0) CNT is considered as a conductor according to the condition of chirality indices (i_1,i_2) i.e. $(i_1\text{-}i_2 = 3p)$, where p is an integer as it appears in Fig. 3(a), which shows the current as it grows linearly at very small values of the applied voltage. It is found out that by applying the

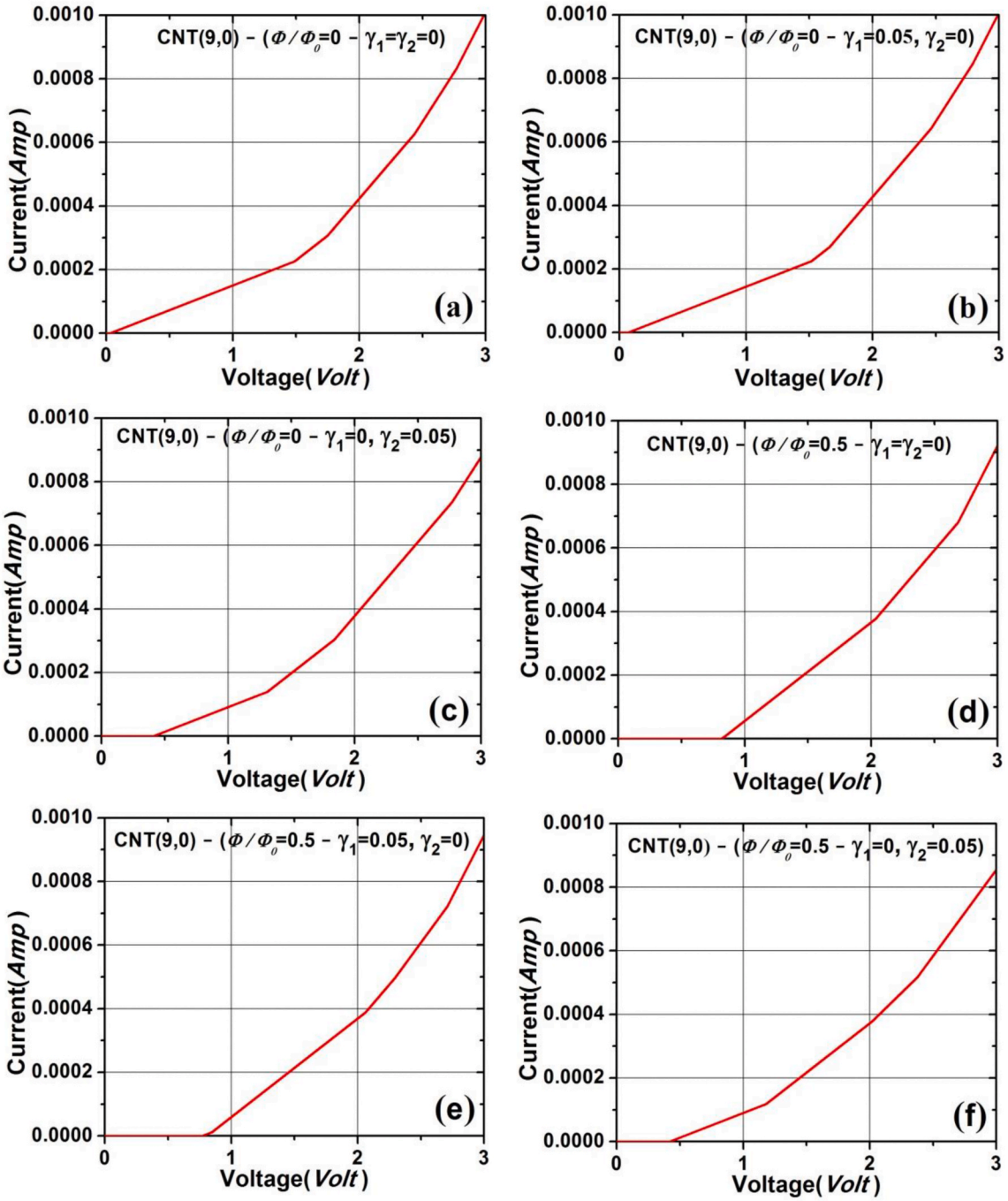

Fig. 3. *I–V* characteristics for zig-zag (9,0) CNT: undeformed with $\Phi/\Phi_0 = 0$ (a), under torsional deformation with $\Phi/\Phi_0 = 0$ (b), under uniaxial deformation with $\Phi/\Phi_0 = 0$ (c), undeformed with $\Phi/\Phi_0 = 0.5$ (d), under torsional deformation with $\Phi/\Phi_0 = 0.5$ (e) and under uniaxial deformation with $\Phi/\Phi_0 = 0.5$ (f).

torsional deformation, zig-zag (9,0) CNT behaves as a semiconductor with a very slight change in the value of the threshold voltage, as illustrated in Fig. 3(b). At a threshold voltage equal to 0.075 V, the electric current begins to grow until it corresponds to the quantum magnetic number $m = 6$ in the energy spectrum of zig-zag (9,0) CNT. And the linear growth of the current continues with two kinks at the voltages equal to 1.52 V and 2.48 V, which represent the second and third channels of conductivity, respectively. Fig. 3(c) shows the *I–V* characteristic of zig-zag (9,0) CNT under the effect of the uniaxial deformation, where it should be noted that the first channel opens at the voltage 0.418 V, while the first and second kinks appear at 1.32 V and 1.85 V, respectively. It can be easily understood that the threshold voltage under the tension deformation is greater than that it is under the torsional deformation by about 34%.

The influence of the external magnetic field is also studied in the absence and presence of deformation, as shown in Fig. 3(d), (e) and (f), respectively. On the other hand, the applied magnetic field significantly enhances the energy gap opening, where it appears clearly it the behavior of the *I–V* characteristics of the zig-zag (9,0) CNT as illustrated in Fig. 3 (d).

So, the magnetic field can modify the conducting CNT to become a semiconductor with an acceptable energy gap, and it requires a threshold voltage equal to 0.816 V. As mentioned above, the torsional deformation has an insignificant effect, so merging this type of deformation with the magnetic field does not offer anything to improve the electronic properties of zig-zag (9,0) CNT (see Fig. 3(e)). It has been emphasized that the effect of the uniaxial tension could dramatically decrease the influence of the magnetic field. It is clear that the threshold voltage is reduced to be equal to 0.425 V, which corresponds to the first conducting channel, and the two kinks appear at the voltages 1.2 V and 2.4 V, as illustrated in Fig. 3(f).

The conductance of zig-zag (9,0) CNT is calculated as a function of the voltage for different values of the uniaxial tension parameter γ_2 without and with the effect of the magnetic field as shown in Fig. 4(a) and (b), respectively. It is observed from Fig. 4(a) that the behavior of the conductance is different at the initial values of voltage which ranges from 0 to 0.4 V. Then, a slight difference is detected in the conductance under the uniaxial tension at a voltage greater than 1.5 V. The threshold voltage can be directly increased from 0.035 V to 0.418 V by increasing the parameter γ_2. The combined effect of the magnetic field and the uniaxial deformation on the conductance is studied of zig-zag (9,0) CNT. It is found as clear in Fig. 4(b) that the conductance decreases and the threshold voltage increases to the value 0.75 V at the magnetic flux equal to $\Phi/\Phi_0 = 0.5$ when the effect of deformation excluded. The values of threshold voltages decrease when the effect of deformation is included simultaneously with the influence of the magnetic field. Fig. 4 (c) demonstrates the relationship between the conductance and the two forms of the studied deformation for zig-zag (9,0) CNT in the absence and presence of a magnetic flux. It appears that the conductance decreases by increasing the uniaxial tension parameter γ_2 without the magnetic flux. On the other hand, there is no significant effect under the torsional deformation in the absence and presence of the magnetic flux for all values of γ_1 which can be seen clearly in Fig. 4(c). The effect of the magnetic flux leads to a remarkable change in the conductance as a

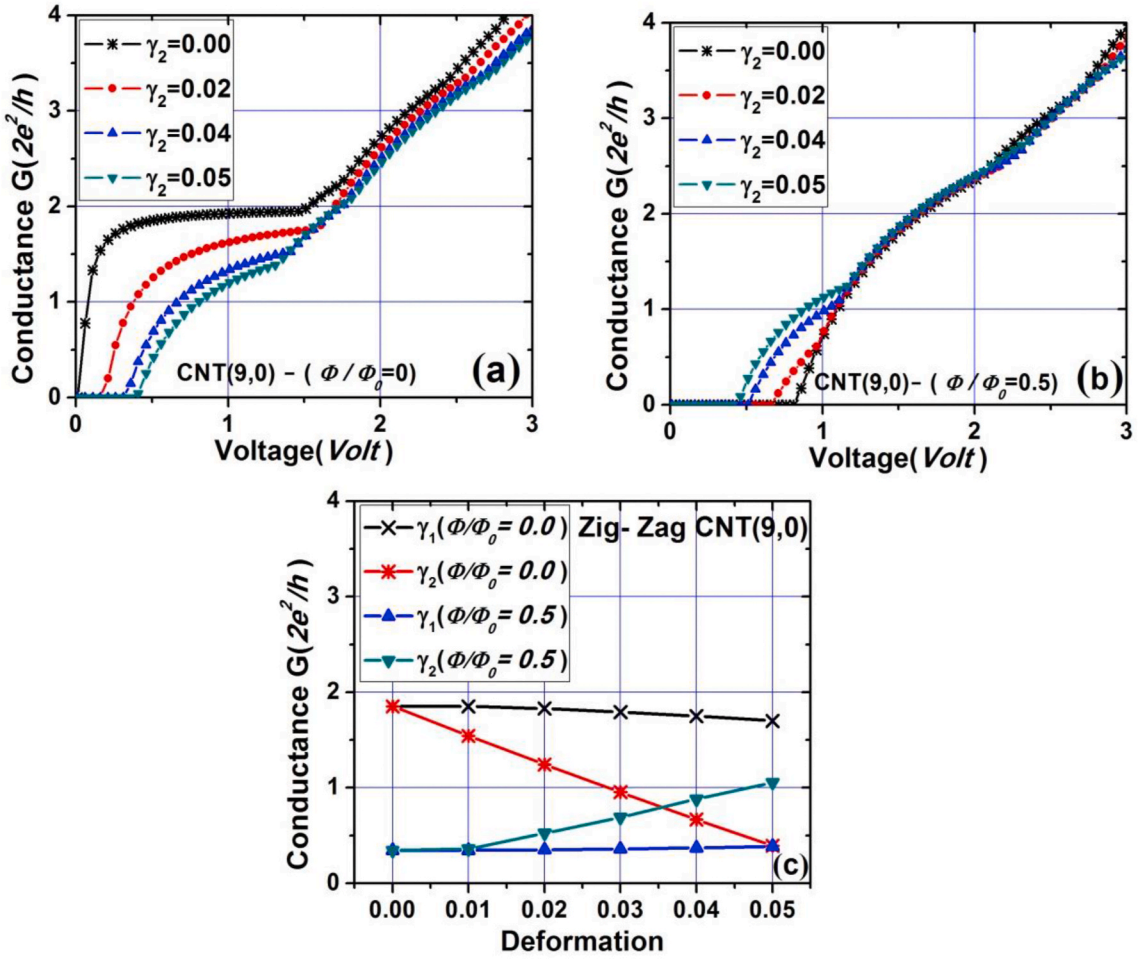

Fig. 4. The conductance dependence on the voltage for zig-zag (9,0) CNT under uniaxial deformation without magnetic flux (a), with magnetic flux (b) and the conductance dependence on the deformation parameters without and with magnetic flux (c).

linear growth with the increasing the parameter γ_2.

Finally, the chiral (15,6) CNT has been included in our present study, which represents a conducting CNT. We have plotted the *I–V* characteristics for the unstrained CNT, CNT under the torsional deformation, under the uniaxial tension, under the effect of magnetic field without deformation, under the effect of magnetic field with a torsional deformation and under the magnetic field with the uniaxial tension in Fig. 5 (a), (b), (c), (d), (e) and (f), respectively. In the absence of the effect of deformation and the magnetic field, it should be noted that the chiral (15,6) CNT behaves as a conductor, where the current begins to flow at the threshold voltage 0.006 V. Consequently, we notice the appearance of the first kink at the voltage 0.75 V; at this voltage a new channel would opened, as evident in Fig. 5(a). Fig. 5(b) shows the chiral (15,6) CNT under the influence of the torsional deformation. It seems that the threshold voltage increases to be equal to 0.282 V, while the first channel opens at voltage 0.5 V. Thus, one can modify the electronic properties of the chiral (15,6) CNT under the influence of the torsional deformation and the conducting CNT becomes a semiconductor. Similar trends have also been observed for the *I–V* characteristics of chiral (15,6) CNT under the effect of the uniaxial tension and the previous deformation as shown in Fig. 5(c), where the threshold voltage appears at 0.286 V and the first kink in the curve is generated at 0.55 V. The similar behavior of the deformation at the value $\gamma_1 = \gamma_2 = 0.05$ is due to the inversion symmetry in the chiral (15,6) CNT. Fig. 5(d) shows a diagram of the undeformed chiral (15,6) CNT when a magnetic field is applied. It also reveals that the lowest conducting band fills at a voltage equal to 0.392 V, which corresponds to the magnetic quantum number $m = 12$. The first kink appears at the voltage 1.19 V, however, this opens a new

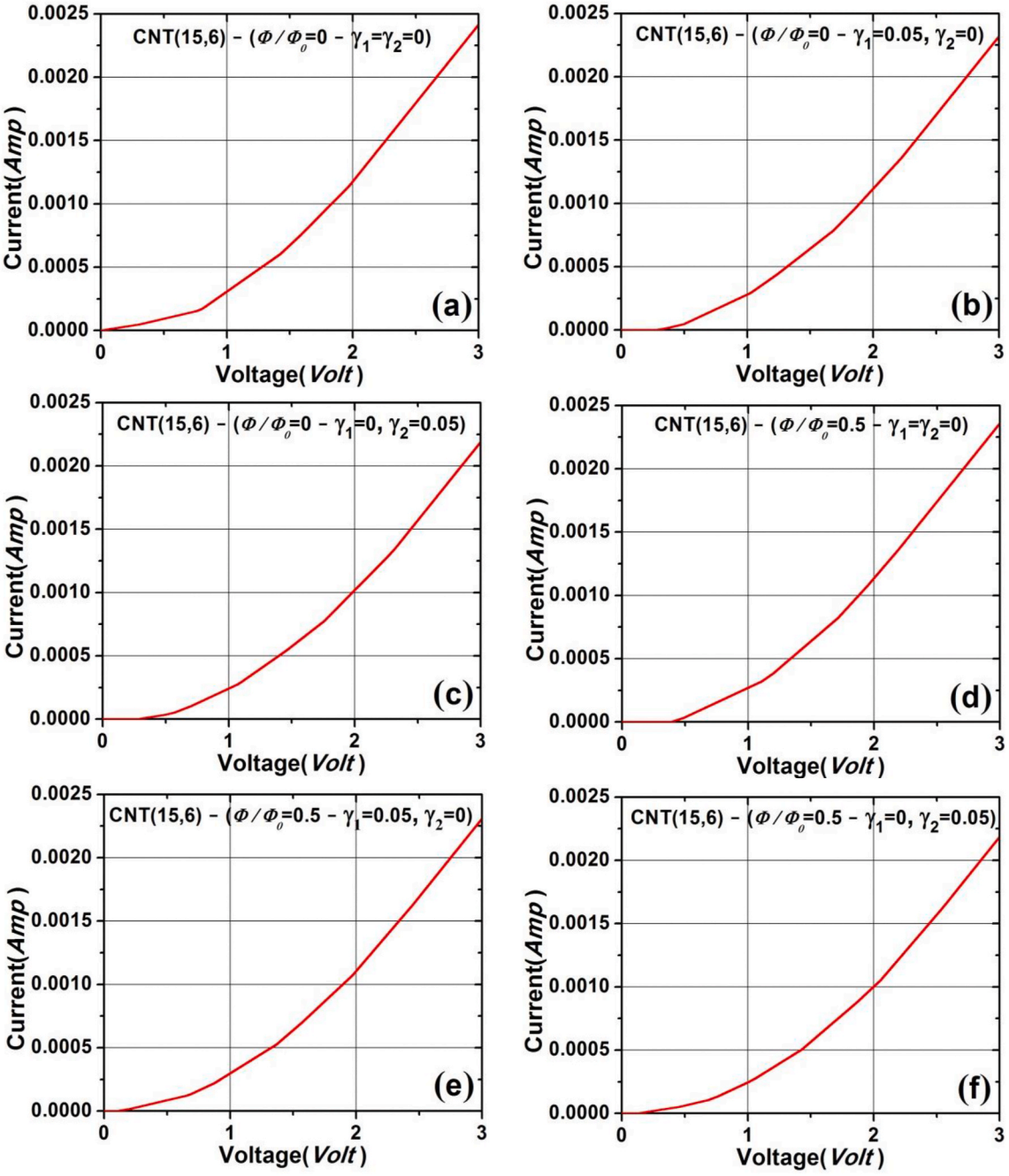

Fig. 5. *I–V* characteristics for chiral (15,6) CNT: undeformed with $\Phi/\Phi_0 = 0$ (a), under torsional deformation with $\Phi/\Phi_0 = 0$ (b), under uniaxial deformation with $\Phi/\Phi_0 = 0$ (c), undeformed with $\Phi/\Phi_0 = 0.5$ (d), under torsional deformation with $\Phi/\Phi_0 = 0.5$ (e) and under uniaxial deformation with $\Phi/\Phi_0 = 0.5$ (f).

channel to help the current flow in the device. It is observed from Fig. 5 (e) and (f), that the curves of the *I–V* characteristics under the torsional deformation and uniaxial tension behave exactly the same when combined with the magnetic field, where the threshold voltage for each of them is 0.107 V and 0.136 V, respectively, and the first kinks occur at voltage values 0.7 V and 0.75 V, respectively.

Correspondingly, we also investigated the conductance of the chiral (15,6) CNT under the torsional and uniaxial deformation as a function of the applied voltage in the absence and presence of an external magnetic field. As mentioned in the previous section about the *I–V* characteristics, the behavior of the conductance does not significantly change under the torsional and uniaxial deformation for all allowed values of the parameters γ_1 and γ_2 as it is evident in Fig. 6 (a) and (b). The combination of the magnetic field with the torsional deformation leads to a significant decrease in the conductance at the initial values of the voltages (see Fig. 6(c)). Consequently, here, the threshold voltage decreased by increasing the parameter γ_1, and it will contribute to the possibility of converting the conducting chiral (15,6) CNT to a semiconductor. On the other hand, it is shown in Fig. 6 (d) that the combination between the magnetic field and the uniaxial tension possesses as similar effect as the

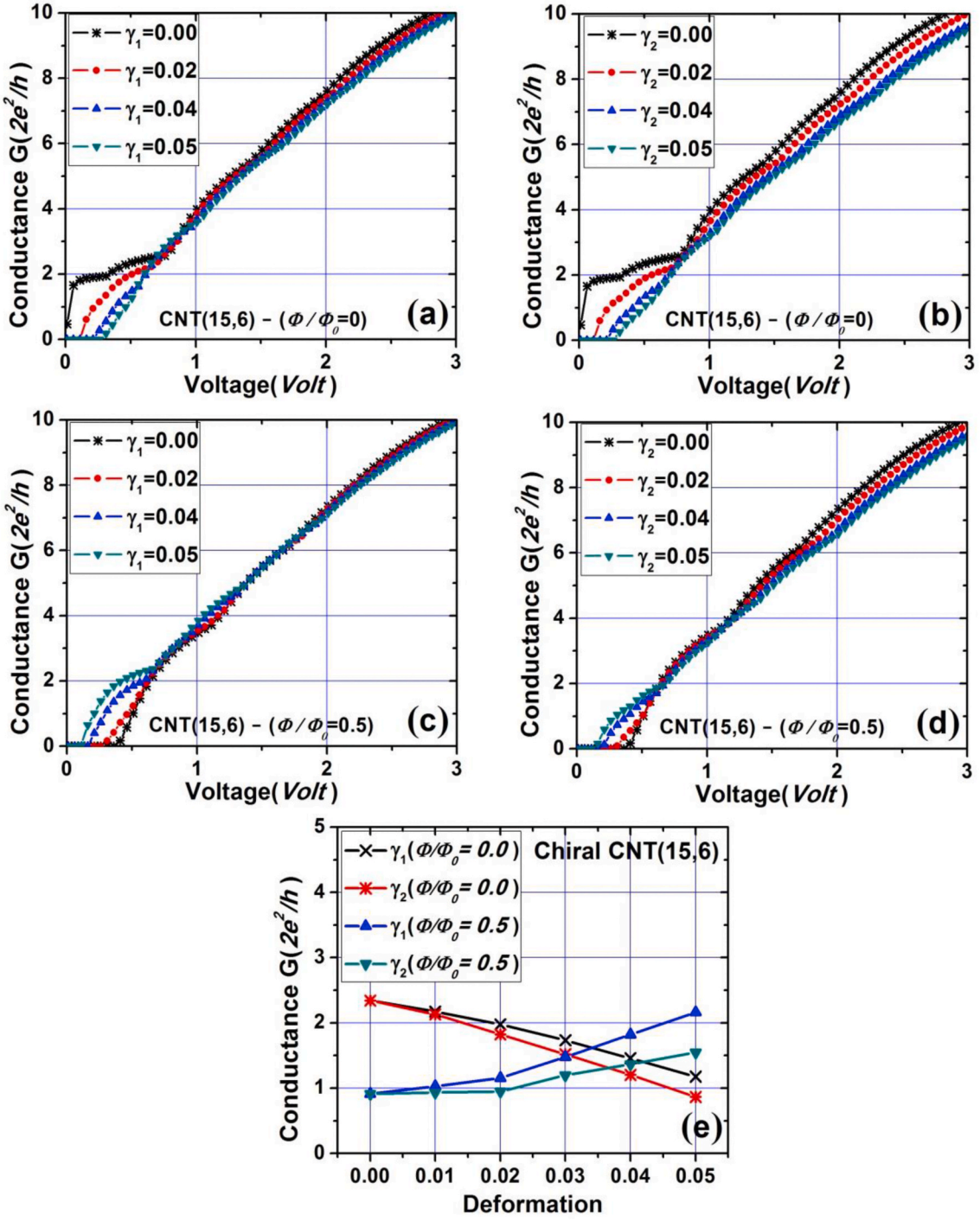

Fig. 6. The conductance dependence on the voltage for chiral (15,6) CNT: under torsional deformation without magnetic flux (a), under uniaxial deformation without magnetic flux (b), under torsional deformation with magnetic flux (c), under uniaxial deformation with magnetic flux (d) and the conductance dependence on the deformation parameters without and with magnetic flux (e).

previous combination with the torsional deformation. As it is clear in Fig. 6, the dominant effect on the electronic and transport properties of the chiral (15,6) CNT results from the effect of the magnetic field.

The conductance dependence on the torsional and uniaxial tension parameters of chiral (15,6) CNT with and without the effect of the magnetic field is plotted in Fig. 6(e). In the absence of the magnetic flux, the conductance decreases linearly by increasing γ_1 and γ_2 to be equal to 1.17 and 0.87, respectively. In the presence of the magnetic flux, the conductance increases apparently with the increase in the parameters γ_1 and γ_2, it means that the magnetic field will inversely alter the effect of the mechanical deformation. Hence, one can readily say that the electronic properties of chiral (15,6) CNT become tunable and more effective by controlling the effect of the mechanical deformation and magnetic field.

4. Conclusions

We have performed detailed calculations to study the effects of the mechanical deformation and the magnetic field on the electronic transport properties of SWCNT, which represents one dimensional material with a variety of electronic properties depending on their intrinsic geometrical structure. We can infer that the adjustable patterns of the mechanical deformation and the magnetic field, applied along the axis of the CNT, may play a vital role to control the position of Dirac points in the reciprocal lattice, and then, to modify the electronic properties of the CNTs. Our study emphasized that the effects of the deformation and magnetic field on the electronic properties of the CNT are very sensitive to the type of structural deformation (torsional or uniaxial) and chirality of CNT. One can also say that the transport properties of CNT depend essentially on the mirror symmetry of the structural lattice, which can be broken under the influence of the mechanical deformation or magnetic field. Moreover, an important result of the present study is that the influence of the applied magnetic field on the CNT may eliminate the effect of the mechanical deformation or increase it according to the chirality of CNT. Finally, our theoretical results confirmed that the mechanical deformation combined with the external magnetic field which applied on the armchair, zig-zag and chiral CNT, is the most promising method to enhance the electronic properties, which contribute to the possibility of developing the nanoelectronic techniques.

5. Author contribution statements

M. J. Majid and A. A. Ali conceived of the presented idea. M. J. Majid developed the theory and performed the computations.

A. A. Ali verified the analytical methods. M. J. Majid encouraged A. A. Ali to investigate the conductance and I–V characteristics for SWCNTs under the influence of the longitudinal magnetic field and mechanical deformation and supervised the findings of this work. All authors discussed the results and contributed to the final manuscript.

Declaration of competing interest

All authors have no conflicts of interest.

Acknowledgments

We gratefully acknowledge support from University of Basrah. We would like to thank Dr. S.S. Savinskii - Udmurt State University for helpful discussions.

References

[1] S. Iijima, Helical microtubules of graphitic carbon, Nature 354 (1991) 56.
[2] F. Leonard, The Physics of Carbon Nanotube Devices, William Andrew Inc., 2008, p. 295.
[3] L. Yang, M.P. Anantram, J. Han, J.P. Lu, Band-gap change of carbon nanotubes: effect of small uniaxial and torsional strain, Phys. Rev. B 60 (1999) 13874.
[4] N. Ma, S. Zhang, D. Liu, V. Wang, Mechanical strain induced valley-dependent quantum magnetotransport of Dirac particles in graphene, Phys. Lett. 379 (2015) 3123.
[5] J. Chen, S. Kumar, Variability in output characteristics of single-walled carbon nanotube thin-film transistors, IEEE Trans Nanotechno 17 (2018) 353.
[6] H. Kang, S.J. Hong, M. Park, H.-S. Jang, K. Nam, S. Choi, B.H. Kim, Y.W. Park, Tuning the electronic structure of single-walled carbon nanotube by high-pressure H_2 exposure, Nanotechnology 30 (2018), 065201.
[7] O.E. Glukhova, D.S. Shmygin, The electrical conductivity of CNT/graphene composites: a new method for accelerating transmission function calculations, Beilstein J. Nanotechnol. 9 (2018) 1254.
[8] G.P. Evans, D.J. Buckley, N.T. Skipper, I.P. Parkin, Switchable changes in the conductance of single-walled carbon nanotube networks on exposure to water vapour, Nanoscale 9 (2017) 11279.
[9] A.E. Champo, P.R. Taboada, G.G. Naumis, Landauer-Büttiker conductivity for spatially-dependent uniaxial strained armchair-terminated graphene nanoribbons, Physica E Low Dimens. Syst. Nanostruct 102 (2018) 123.
[10] M.J. Majid, B.K. Najlaa, S.S. Savinskii, Modification of electronic properties of graphene under three patterns of elastic deformation, Indian J. Phys. 92 (2018) 159.
[11] I.D. Aditya, S. Widayani, S. Suprijadi, Electronic properties of semi conducting zigzag (10,0) carbon nanotubes due to uniaxial strain, ARPN : JEAS 13 (2018) 2390.
[12] Y. Kuwahara, T. Hirai, T. Saito, Effects of tube diameter and length on transparent conductivity of single-walled carbon nanotube network films, J. Nanomater. 2018 (2018) 1.
[13] F. Muttaqien, S. Suprijadi, Ab initio study of semiconductor atoms impurities in zigzag edge (10,0) carbon nanotubes, AIP Conf. Proceed. 1656 (2015), 060006.
[14] P. Szroeder, I.Y. Sagalianov, T.M. Radchenko, V.A. Tatarenko, Y.I. Prylutskyy, W. Strupinski, Effect of uniaxial stress on the electrochemical properties of graphene with point defects, Appl. Surf. Sci. 442 (2018) 185.
[15] M.J. Majid, *I–V* characteristics and conductance of strained SWCNTs, Phys. Lett. 383 (2019) 879.
[16] M.J. Majid, S.S. Savinsky, Change in the electronic spectrum of a carbon nanotube during elastic deformation and the relative shear of atomic sublattices, Tech. Phys. 57 (2012) 726.
[17] M.J. Majid, S.S. Savinskii, Variation of electron spectrum of elastically plane-strained graphene, Tech. Phys. Lett. 37 (2011) 519.
[18] G.G. Naumis, P.R. Taboada, Mapping of strained graphene into one-dimensional Hamiltonians: quasicrystals and modulated crystals, Phys. Rev. B 89 (2014) 241404 (R).
[19] S. Zaric, G.N. Ostojic, J. Kono, J. Shaver, V.C. Moore, M.S. Strano, R.H. Hauge, R. E. Smalley, X. Wei, Optical signatures of the Aharonov–Bohm phase in single-walled carbon nanotubes, Science 304 (2004) 1129.
[20] A. Javey, J. Kong, Carbon Nanotube Electronics, Springer, 2009, p. 274.
[21] S.S. Savinskii, A.V. Belosludtsev, Conductance of a single-wall carbon nanotube in a one-parameter tight-binding model, Phys. Solid State 46 (2004) 1376.
[22] E. Faizabadi, Z. Kargar, Effects of uniaxial strain on quantum conductance of finite zigzag single wall carbon nanotubes, Proc. SPIE 8101 (2011) 81010V.
[23] M.J. Majid, B.K. Najlaa, Band structure variation for SWCNTs under deformation, J. Basrah Res. (Sci.) 43 (2017) 1.